Liquid Crystals
Publication details, including instructions for authors and subscription information:
http://www.informaworld.com/smpp/title~content=t713926090

Polar phases in chiral thiobenzoate liquid crystals

P. Simeão Carvalho[a]; M. Glogarová[ab]; M. R. Chaves[a]; H. T. Nguyen[c]; C. Destrade[c]; J. C. Rouillon[c]; S. Sarmento[a]; M. J. Ribeiro[a]
[a] Departamento de Fisica, Faculdade de Ciẽncias da Universidade do Porto, Centro de Fisica da Universidade do Porto, Instituto Materials (IMAT-Núcleo IFIMPU), Porto, Portugal [b] Institute of Physics, Academy of Sciences of the Czech Republic, Prague, Czech Republic [c] Centre de Recherche Paul Pascal, Pessac, France

To cite this Article Carvalho, P. Simeão , Glogarová, M. , Chaves, M. R. , Nguyen, H. T. , Destrade, C. , Rouillon, J. C. , Sarmento, S. and Ribeiro, M. J.(1996) 'Polar phases in chiral thiobenzoate liquid crystals', Liquid Crystals, 21: 4, 511 — 521
To link to this Article: DOI: 10.1080/02678299608032859
URL: http://dx.doi.org/10.1080/02678299608032859

LIQUID CRYSTALS, 1996, VOL. 21, NO. 4, 511–521

Polar phases in chiral thiobenzoate liquid crystals

by P. SIMEÃO CARVALHO†, M. GLOGAROVÁ§†, M. R. CHAVES†, H. T. NGUYEN‡, C. DESTRADE‡, J. C. ROUILLON‡, S. SARMENTO† and M. J. RIBEIRO†

†Departamento de Física, Faculdade de Ciências da Universidade do Porto, Centro de Física da Universidade do Porto, Instituto Materials (IMAT-Núcleo IFIMPU), Rua do Campo Alegre 687, 4150 Porto, Portugal

‡Centre de Recherche Paul Pascal, Av. Schweitzer, 33600 Pessac, France

§Institute of Physics, Academy of Sciences of the Czech Republic, Na Slovance 2, 180 40, Prague 8, Czech Republic

(*Received 25 January 1996; in final form 16 April 1996; accepted 1 May 1996*)

By dielectric measurements, the temperature scan method and studies of optical hysteresis loops, the phase sequences have been elucidated for two new compounds from a series of homologues containing a thiobenzoate group with a fluoro substituent in the first benzene ring (denoted *n*FHTBBM7*). Both compounds ($n = 11$ and $n = 12$) exhibit antiferroelectric ($S^*_{C_A}$), ferroelectric (S^*_C) and several ferrielectric ($S_{C_{FI}}$) phases, as well as the ($S^*_{C_\varepsilon}$) phase. Also, in the compound 11FHTBBM7*, a metastable ferrielectric phase may appear in the temperature range of the antiferroelectric phase. The dielectric relaxation study revealed contributions to the dielectric constant from several modes detected in the temperature range studied. The properties of the relaxation modes and the phase transition sequences of the two compounds have been compared with those of the homologues with $n = 9$ and $n = 10$ studied previously.

1. Introduction

Chiral liquid crystal materials with a thiobenzoate group are known to exhibit $S^*_{C_\varepsilon}$, ferro-, ferri- and antiferro-electric mesophases [1–5]. Here we present the study of two compounds possessing a thiobenzoate group with a fluoro substituent in the first benzene ring, having the general chemical formula

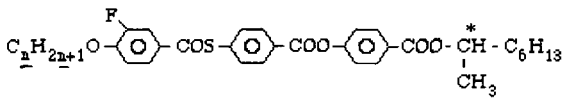

and denoted as *n*FHTBBM7*, where $n = 11$ and $n = 12$. The compounds from this series with $n = 9$ and $n = 10$ have been studied previously [3, 4].

The first assessment of the mesomorphic properties of the compounds studied was made by DSC measurements and texture observations. The phase sequences between the crystalline (Cr) and the isotropic (I) phases and the corresponding transition temperatures on heating suggested for 11FHTBBM7* were:

$$\text{Cr } 73^\circ\text{C } S^*_{C_A} \ 85^\circ\text{C } S^*_{C_{FI2}} \ 89^\circ\text{C } S^*_{C_{FI1}} \ 94^\circ\text{C } S^*_C$$
$$117^\circ\text{C } S_A \ 132^\circ\text{C I}$$

and for 12FHTBBM7*:

$$\text{Cr } 63^\circ\text{C } S^*_{C_A} \ 97^\circ\text{C } S^*_{C_{FI1}} \ 101^\circ\text{C } S^*_C \ 119^\circ\text{C } S_A \ 131^\circ\text{C I}.$$

In this paper we present the results found from dielectric relaxation studies, from switching studies made by means of optical hysteresis loops and from the temperature scan method (TSM) [5]. The results obtained have enabled elucidation of the phase sequence between the antiferroelectric phase and the S_A phase. The differences and similarities found for the two compounds are discussed, compared with the results obtained previously for the compounds with $n = 9$ and 10 [3, 4] and related to the influence of the alkoxy chain length.

2. Experimental

The liquid crystals were filled into commercial cells with a spacing of 25 μm. The sample alignment was evaluated by optical observations. The complex dielectric constant ($\varepsilon', \varepsilon''$) was measured either at a constant frequency during continuous heating and cooling runs at a rate of $1{\cdot}2\ \text{K min}^{-1}$ or at stabilized temperatures while changing the frequency from 20 Hz to 1 MHz. The measuring a.c. field was $0{\cdot}01\ \text{V μm}^{-1}$.

The optical hysteresis loops were obtained by measuring the transmitted light intensity I_t with a photodiode attached to a polarizing microscope. A halogen lamp was used as a light source. The loops were recorded during sample switching with triangular waves, with a

frequency from 0·2 Hz ($S^*_{C_A}$) to 1 Hz ($S^*_{C_\alpha}$) for $n = 11$ and from 0·1 Hz ($S^*_{C_A}$) to 25 Hz ($S^*_{C_\alpha}$) for $n = 12$.

The temperature scan method (TSM) [5] was used to disclose the polar phases. A 1 kHz square wave electric field was applied to the sample during heating runs at a constant rate of 1·2 K min^{-1}. The electric current density J flowing through the sample during the temperature runs,

$$J = \frac{\partial \varepsilon}{\partial T}\frac{dT}{dt}E + \varepsilon\frac{dE}{dt} + \frac{\partial P_s}{\partial t} + \frac{\partial P_s}{\partial T}\frac{dT}{dt} + \frac{\partial P_s}{\partial E}\frac{dE}{dt} + \sigma E_l$$
$$= J_i + J_s + J_\lambda + J_E + J_c,$$

consists of contributions from the dielectric constant of the sample (J_i), polarization switching (J_s), pyroelectric effect (J_λ), wave form of the applied field (J_E) and ionic current (J_c). In this expression, ε is the permittivity, P_s the polarization imposed by the macroscopic field E and E_l the local field, which is a function of the switched polarization P_s. The time average current $\langle I \rangle$ flowing in the circuit was measured by an electrometer, as a voltage on a resistor in series with the sample. The full description of this method was given in [5].

All the measurements on heating runs were made after cooling from the I phase but without going into the crystalline phase.

3. Results and discussion

3.1. *Results for 11FHTBBM7**

The study of 11FHTBBM7* revealed a very complex behaviour, which makes the analysis of the experimental results difficult. As can be seen in figures 1(*a*) and 1(*b*) the temperature dependence of the real part of the dielectric constant (ε'), measured on cooling and heating runs, presents an anomalous thermal hysteresis of about 8 K. On heating runs the results are very reproducible except for the temperature range below 73 K.

In several repeated cooling runs, we may distinguish two types of behaviour which we classify as type I and type II. A maximum around 80°C appears for type I behaviour but is not observed in type II. As a consequence, on further cooling, ε' takes higher values in type I than in type II. When type I behaviour occurs, then on subsequent heating (figure 1(*b*)), ε' falls between 70°C and 73°C to the same value that is measured for type II behaviour at that temperature. We must point out that this jump in $\varepsilon'(T)$, only seen on the type I curve, is not related to a phase transition and it will be explained below. Above 73°C, on heating runs, $\varepsilon'(T)$ values for both types I and II exhibit no significant differences.

For the determination of the phase transition temperatures and phase assignment, only $\varepsilon'(T)$ from heating runs were considered, because on cooling, the phase transitions are not clearly seen. On heating, reproducible anomalies in $\varepsilon'(T)$ can be observed in figure 1(*b*) at 84°C, 90°C and 94°C and are indicated by the dashed lines. These temperatures, related to phase transitions, are close to those obtained by DSC (85°C, 90°C and 94°C, respectively).

The maximum around 110°C does not correspond to a phase transition, but occurs within the S^*_C phase, as has been frequently observed [4, 6] and is related to the temperature effect on the helix pitch [6, 7]. The transition temperature to the S_A phase, which could not be inferred from $\varepsilon'(T)$, was determined by the DSC measurements and occurs at 117°C.

The average current response, measured by the temperature scan method [5] under an a.c. electric field of 0·6 V μm^{-1} is depicted in figure 2 and shows the existence of several steps. In the description of this method [5], it has been shown that these steps may correspond to different polar phases. The low current response in the low temperature region corresponds to the antiferroelectric phase ($S^*_{C_A}$). Between this phase and the S^*_C phase, three steps on the current response occur over reproducible temperature ranges. We suggest that these steps correspond to three ferrielectric phases (denoted $S^*_{C_{FI3}}$, $S^*_{C_{FI2}}$ and $S^*_{C_{FI1}}$), as indicated in figure 2. Two of them ($S^*_{C_{FI2}}$ and $S^*_{C_{FI1}}$) have also been detected from the dielectric measurements (see figure 1(*b*)) and by texture observations on homeotropic cells. The temperature range of the $S^*_{C_{FI3}}$ phase is clearly identified by the anomalies in TSM at ≈76°C and 85°C, although there is no clear evidence for this phase from the DSC and ε' measurements.

From the DSC study and texture observations, the low temperature limit of the S_A phase was found at 117°C, but from the results shown in figure 2 one can see that the high limit of the S^*_C phase takes place at 114°C. As there is a close agreement between the phase transition temperatures $S^*_{C_A}$–$S^*_{C_{FI2}}$–$S^*_{C_{FI1}}$–S^*_C obtained from DSC and those obtained from the dielectric and TSM measurements, it is not expected that the transition temperature to the S_A phase is significantly different from that obtained by DSC measurements. Therefore, the existence of the $S^*_{C_\alpha}$ phase can be proposed in the 114–117°C temperature range. The transition to the S_A phase was not however detected by TSM measurements, probably due to the weak polar character of the $S^*_{C_\alpha}$ phase in this compound.

Quasi-static optical hysteresis loops, recorded for each phase and presented in figure 3, help to confirm the polar character of the assigned phases. In all the phases, the applied field was strong enough to induce the saturated ferroelectric state. The loop recorded for the low temperature phase (figure 3(*a*)) shows an antiferroelectric switching, characterized by a high threshold

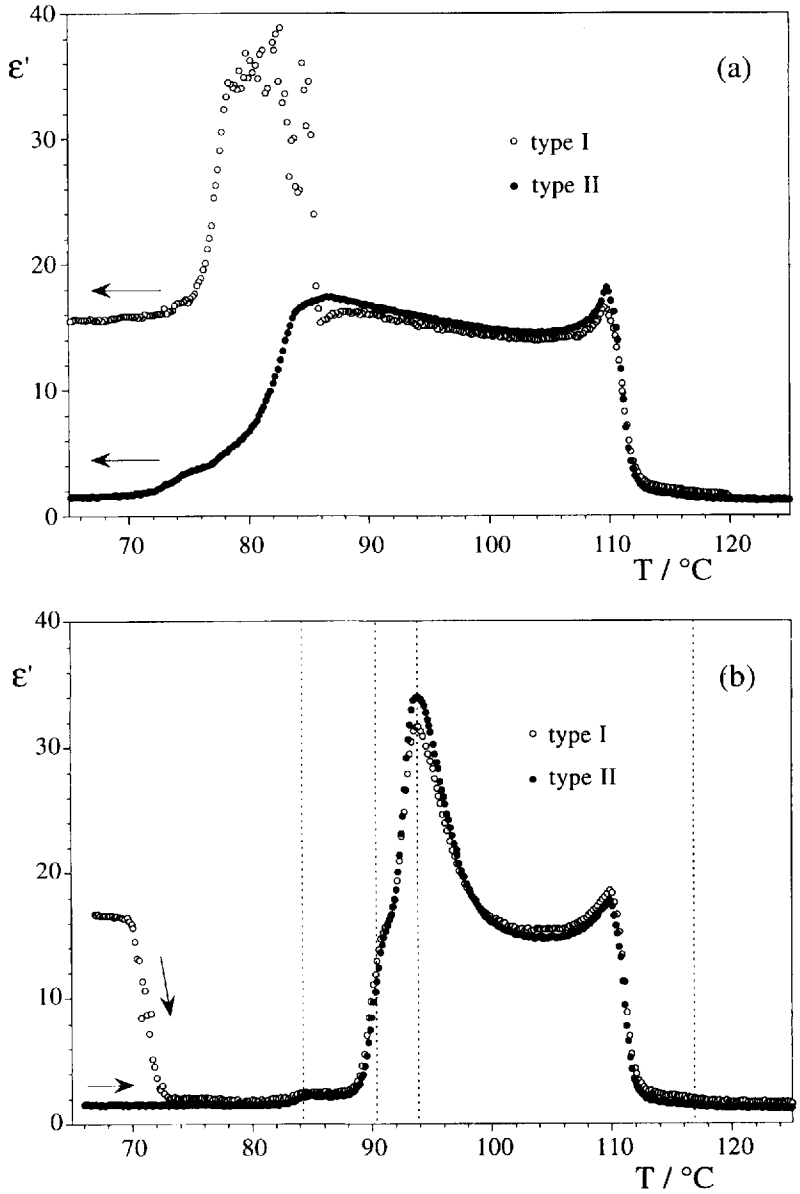

Figure 1. Temperature dependence of the real part of the dielectric constant measured for 11FHTBBM7* in (*a*) cooling and (*b*) heating runs at a frequency of 80 Hz. The dashed lines indicate phase transition temperatures.

field. The peaks observed at zero field in figure 3 (*a*)), which are attenuated when the frequency of the field is lowered, are probably due to ferroelectric-like switching which takes place near the surfaces, where the antiferroelectric structure may be restored more slowly. The three loops recorded for the phases denoted as $S^*_{C_{FI3}}$, $S^*_{C_{FI2}}$ and $S^*_{C_{FI1}}$, exhibit intermediate states induced by the electric field (figures 3 (*b*), 3 (*c*) and 3 (*d*)), which confirm the ferrielectric character of these phases. The loop recorded for the $S^*_{C_{FI3}}$ phase can be distinguished from those recorded for the other two phases by the high value of the full switching field ($E_s \approx 2{\cdot}4\,V\,\mu m^{-1}$) which is similar to that for the $S^*_{C_A}$ phase ($\approx 2{\cdot}8\,V\,\mu m^{-1}$), but different from the switching field for the $S^*_{C_{FI2}}$ and $S^*_{C_{FI1}}$ phases (1·1 and 1·2 $V\,\mu m^{-1}$, respectively). Although the loop in figure 3 (*b*) could suggest that the $S^*_{C_{FI3}}$ phase could result from the coexistence of the $S^*_{C_A}$ and $S^*_{C_{FI2}}$ phases, the current steps observed by TSM measurements at 76°C and at 85°C (figure 2) do not exclude the possible existence of a different ferrielectric ($S^*_{C_{FI3}}$) phase. All the measurements suggesting the existence of the $S^*_{C_{FI3}}$ phase (TSM and hysteresis loops) were made with

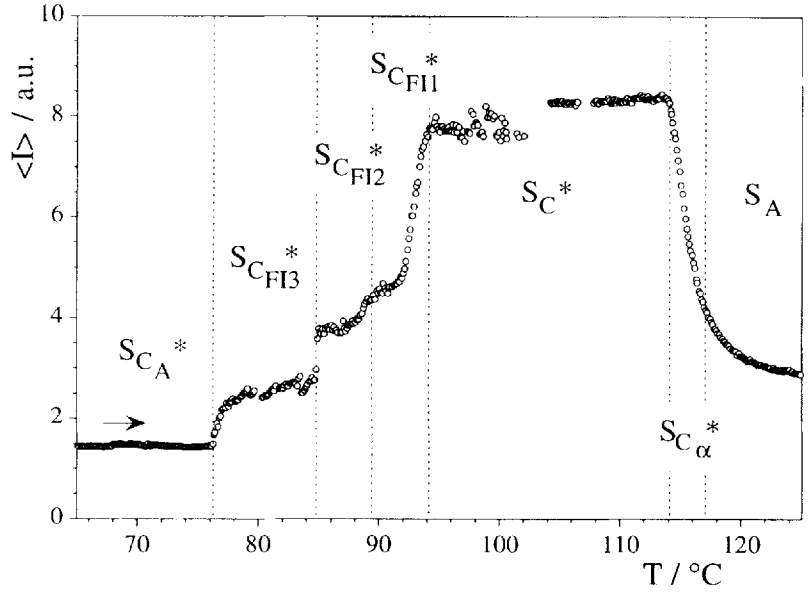

Figure 2. Average current intensity measured by TSM for 11FHTBBM7* under a field of 0·6 V μm^{-1}. The dashed lines indicate phase transitions between the different phases.

a high applied field, while those without an applied field reveal no information about this phase. One may conclude that either the $S^*_{C_{FI3}}$ phase exists and is distinguished from the $S^*_{C_A}$ phase only under an applied field or that this phase is induced by the electric field.

The loops recorded for the $S^*_{C_{FI2}}$ and $S^*_{C_{FI1}}$ phases (figures 3(*c*) and 3(*d*)) are similar but can be distinguished by the number of intermediate states induced by the electric field (two and one, respectively). Due to these similar switching properties, the current detected by TSM shows only a small increase at the phase transition between the $S^*_{C_{FI2}}$ and $S^*_{C_{FI1}}$ phases, as seen in figure 2. The main property which distinguishes these two phases is the dielectric response, which is more than five times higher in the $S^*_{C_{FI1}}$ phase than in the $S^*_{C_{FI2}}$ phase (see figure 1(*b*)). The loop shown in figure 3(*e*) is a typical ferroelectric hysteresis loop. Within the 114–117°C temperature range, a non-saturated hysteresis loop was found (figure 3(*f*)) which is characteristic of the $S^*_{C_\alpha}$ phase. Similar loops have been observed for this phase with another compound of the same series [3].

To understand the dielectric behaviour in the antiferro- and ferri-electric phases, a dielectric relaxation study has been made. The relaxation strength ($\Delta\varepsilon$), determined from measurements taken on heating by the Cole–Cole analysis of different modes that contribute to ε' in the temperature range studied, is plotted in figure 4(*a*), for type I behaviour. Those contributions are similar for both type I and type II behaviours except below 73°C, as previously shown (figure 1(*b*)). The line corresponding to the $S^*_{C_A}$–$S^*_{C_{FI3}}$ transition temperature was taken from figure 2. Figure 4(*b*) shows the temperature contribution of the Goldstone mode, obtained for type II behaviour on a cooling run. It is seen that this contribution remains in the ferrielectric and antiferroelectric phases and is responsible for the rather high value of ε' for these phases (see figure 1(*a*)). This behaviour may be due to some kind of ferroelectric order that persists in the sample during cooling. In the low temperature region of the $S^*_{C_A}$ phase, its contribution is no longer observed. For type I behaviour, a mode with the same relaxation frequency ($f_r \approx 3$–4 kHz) as that of the Goldstone mode (see figure 4(*a*)) is observed in the low temperature region of the $S^*_{C_A}$ phase, giving a relatively high contribution to ε'. This result can be interpreted in terms of a metastable phase existing in the low temperature range of this phase. The stabilization of the $S^*_{C_A}$ phase occurs on further heating and is manifested by the jump down of ε' (shown on the type I curve in figure 1(*b*)), between 70°C and 73°C. We are not able to offer a clear explanation of the reasons for this behaviour.

On heating, a low frequency mode ($f_r \approx 150$ Hz) systematically appears between 91°C and 96°C, giving the most important contribution to ε' in this temperature region. This low frequency mode is responsible for the maximum in the real part of the dielectric constant at ≈94°C (figure 1(*b*)). Within the $S^*_{C_{FI2}}$ and $S^*_{C_{FI3}}$ phases, the Goldstone mode has not been detected on heating because, due to its low contribution, it has been masked by the conductivity at the low frequency range.

In the $S^*_{C_A}$ and $S^*_{C_{FI2}}$ phases, a high frequency mode

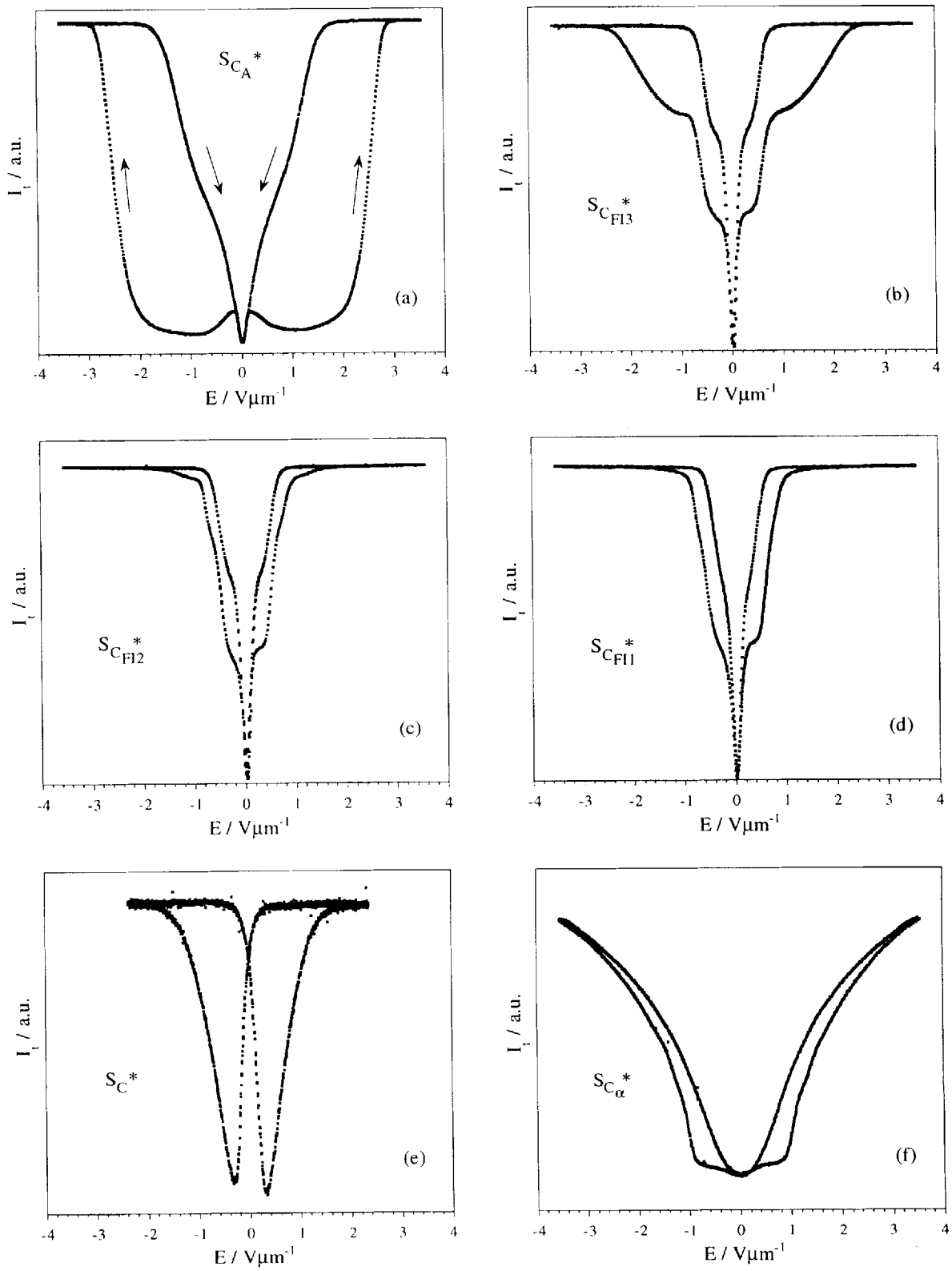

Figure 3. Optical hysteresis loops recorded for 11FHTBBM7* at (*a*) 64°C, (*b*) 78°C, (*c*) 88°C, (*d*) 91°C, (*e*) 98°C and (*f*) 116·5°C. The phases are indicated for each loop.

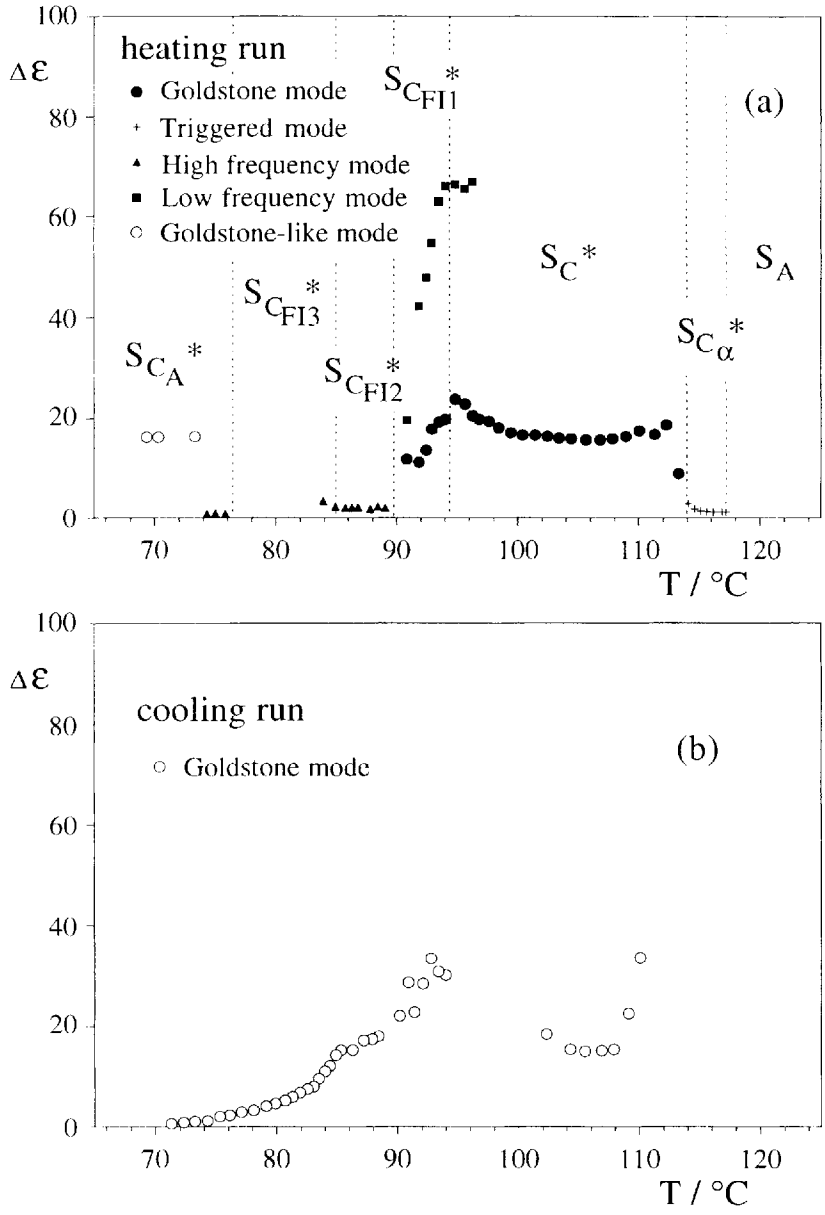

Figure 4. Dielectric relaxation strength $\Delta\varepsilon$ of 11FHTBBM7*, (*a*) for modes contributing to ε^* on heating and (*b*) for the Goldstone mode contribution on cooling. The line corresponding to the $S_{C_A}^*$–$S_{C_{FI3}}^*$ transition was taken from figure 2.

with a nearly constant relaxation frequency of 160 kHz and very low $\Delta\varepsilon$, has been detected on heating runs (figure 4(*a*)). This mode may be either related to the rotation of molecules around their short axes or to the non-collective azimuthal mode [3, 8] which is supposed to exist in all tilted smectic phases [3].

In the $S_{C_\alpha}^*$ phase, another mode has been detected. Its contribution decreases with increasing temperature. It may be related to the mode that has been found for the compound $n = 9$ [3], which is supposed to be triggered by the softening of the fluctuations of the molecular tilt (so-called soft mode) at the S_A–$S_{C_\alpha}^*$ transition. For the compound $n = 9$, this mode was also detected in the ferroelectric phase and exhibited a maximal contribution at the S_C^*–$S_{C_\alpha}^*$ phase transition. It has been suggested [4] that this mode does not correspond to the amplitude fluctuation of the molecular tilt, because this has a maximal dielectric contribution at the transition between the S_A phase and the tilted (S_C^* or $S_{C_\alpha}^*$) phases. The origin of the triggered mode is not known, but we suppose that it is responsible for the onset of the $S_{C_\alpha}^*$ phase.

3.2. *Results for 12FHTBBM7**

Figure 5 shows the temperature dependence of the real part of the dielectric constant, for heating and cooling runs. Similarly to 11FHTBBM7*, the phase assignment has been decided from heating runs only. The anomalies observed at ≈97°C and 101°C are related to phase transitions, in good accordance with the DSC phase assignment. The maximum around 116°C is not related to a phase transition, but occurs within the S_C^* phase, as observed for 11FHTBBM7*. The phase transitions indicated by dashed lines in figure 5 correspond to the heating run. The line at 119°C represents the transition to the S_A phase, determined by DSC measurements. Thermal hysteresis in the dielectric constant is only observed for the low temperature phase transitions.

The TSM results obtained for increasing temperatures, under different a.c. electric fields, are presented in figure 6. The low field curve yields the identification of the ferroelectric S_C^* phase between 101°C and 117°C and of a ferrielectric phase, denoted as $S^*_{C_{FI1}}$, between 97°C and 101°C. A small kink observed on the steep decrease in the TSM current around 118°C may be related to the existence of the $S^*_{C_\alpha}$ phase, which in this compound is clearly revealed under the higher applied field, between the two anomalies at 117°C and 119°C. The higher field curve discloses another ferrielectric phase ($S^*_{C_{FI3}}$) above 93°C, but the $S^*_{C_{FI1}}$–S_C^* phase transition is not seen on this curve as a consequence of the high value of the electric field [5]. The phase transitions revealed by TSM are shown in figure 6 by the dashed lines. The ferrielectric phases ($S^*_{C_{FI3}}$ and $S^*_{C_{FI1}}$) revealed by TSM in 12FHTBBM7* have identical properties to those of the corresponding $S^*_{C_{FI3}}$ and $S^*_{C_{FI1}}$ phases observed for 11FHTBBM7*, as will be explained below.

The optical hysteresis loops obtained for increasing temperatures clearly distinguish the antiferroelectric $S^*_{C_A}$ from the ferrielectric $S^*_{C_{FI3}}$ phase. Figures 7(*a*) and 7(*b*) present the loops obtained for these phases. In the $S^*_{C_{FI1}}$ phase, characterized by significantly higher values of ε' than those for the $S^*_{C_{FI3}}$ phase, the optical hysteresis loop (figure 7(*c*)) exhibits one intermediate state and differs from the loop for the other ferrielectric phase (figure 7(*b*)) which has two intermediate states and a higher full switching field. The switching properties of these two ferrielectric phases, as well as the dielectric responses and the textures observed in homeotropic and planar aligned cells, are similar to those reported for the corresponding phases of 11FHTBBM7*. The $S^*_{C_{FI3}}$ phase is observed only in experiments when a high electric field is applied, in a similar way to that found for 11FHTBBM7*. The characteristic non-saturated loop in figure 7(*d*) was obtained for the $S^*_{C_\alpha}$ phase.

The relaxation strength ($\Delta\varepsilon$) of the modes which contribute to the dielectric constant in the polar phases and of the soft mode in the S_A phase, are shown in figure 8. These data have been obtained from measurements taken for increasing temperatures. In this figure, the line corresponding to the $S^*_{C_A}$–$S^*_{C_{FI3}}$ transition temperature was taken from figure 6. Similarly to 11FHTBBM7*, there is a contribution of the so-called triggered mode in the $S^*_{C_\alpha}$ phase and a contribution of the Goldstone mode in the S_C^* phase with the relaxation

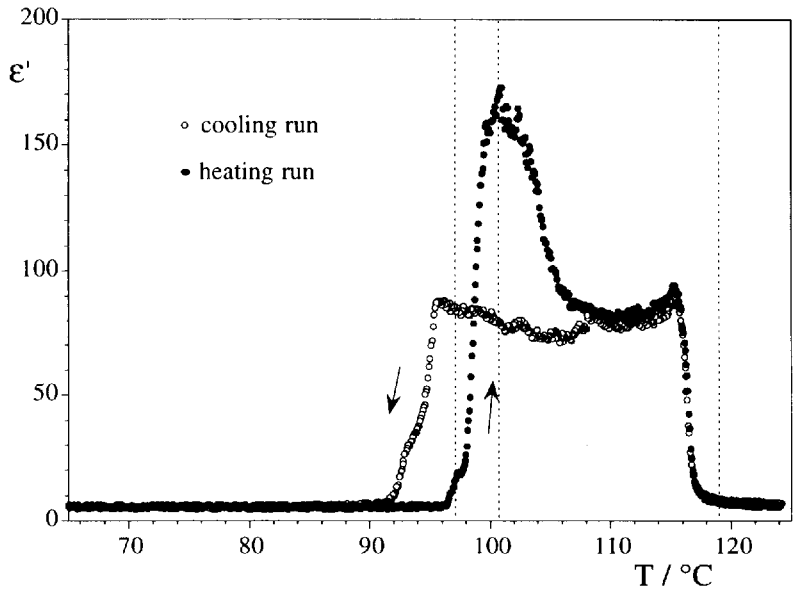

Figure 5. Temperature dependence of the real part of the dielectric constant measured for 12FHTBBM7* at a frequency of 20 Hz. The dashed lines indicate phase transition temperatures on heating.

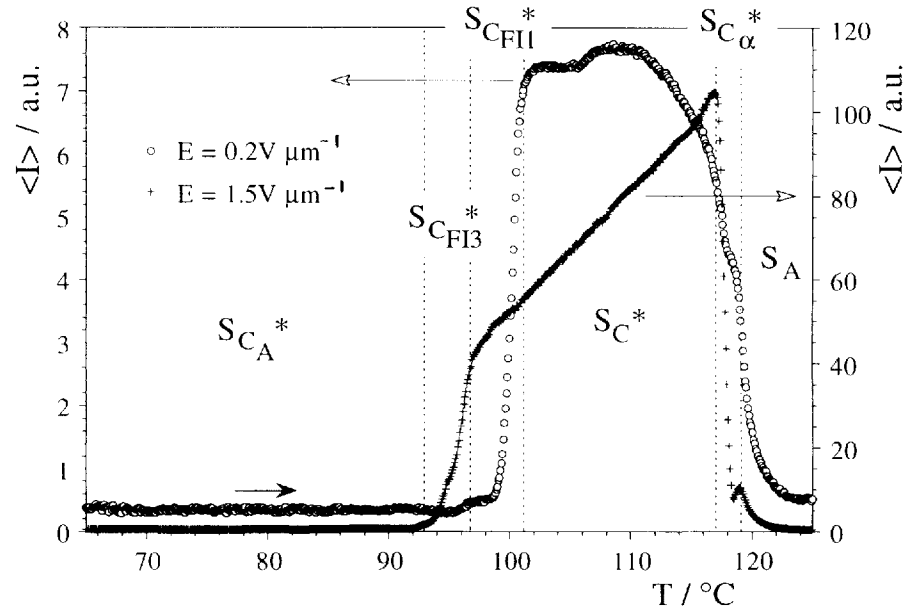

Figure 6. Average current intensity measured by TSM for 12FHTBBM7* under two measuring fields. The dashed lines indicate transitions between the different phases.

frequency $f_r \approx 2$–$3{\cdot}5$ kHz. In the S_C^* phase, near its low temperature limit and in the $S_{C_{FI1}}^*$ ferrielectric phase, there is a high contribution of the low frequency mode ($f_r \approx 100$–500 Hz), which overwhelms the Goldstone mode contribution in this temperature region. The contribution from the high frequency mode ($f_r \approx 15$–50 kHz) is seen in the $S_{C_{FI3}}^*$ phase and a few degrees into the temperature interval of the $S_{C_A}^*$ phase.

4. Comparison of the compounds and conclusions

For both compounds 11FHTBBM7* and 12FHTBBM7*, the phase sequences have been determined only for heating runs. A large thermal hysteresis occurs at low temperatures and the phase transitions existing in that region are smeared on the cooling runs. The experimental results clearly show that both compounds exhibit an antiferroelectric phase at low temperatures and a broad ferroelectric phase at higher temperatures. In both compounds, two ferrielectric phases, $S_{C_{FI1}}^*$ and $S_{C_{FI3}}^*$, have been found. On heating, the dielectric constant in the $S_{C_{FI3}}^*$ phase is as low as that in the $S_{C_A}^*$ phase, but TSM measurements and optical hysteresis loops show different characteristics in those phases. As the $S_{C_{FI3}}^*$ phase was observed only under an applied electric field, it cannot be excluded that this phase is induced by this field.

In 11FHTBBM7*, an additional ferrielectric $S_{C_{FI2}}^*$ phase exists with a polar character close to that of the ferrielectric $S_{C_{FI1}}^*$ phase. The existence of the $S_{C_{FI2}}^*$ phase is also confirmed by DSC measurements, by texture observations and by switching behaviour. In 12FHTBBM7*, this phase has not been observed.

A metastable phase, probably with a ferrielectric character, may exist in 11FHTBBM7* in the temperature region of the $S_{C_A}^*$ phase and is related to a type I behaviour of $\varepsilon'(T)$. This metastable phase is probably the origin of the intermediate state observed in the optical hysteresis loop for this phase; this has not been observed on the loop for the $S_{C_A}^*$ phase of 12FHTBBM7* (cf. figures 3(*a*) and 7(*a*)).

From the dielectric study, we can obtain some information about the origin of the phase sequences. The maximum of ε' at the $S_{C_{FI1}}^*$–S_C^* transition is caused by the contribution of a mode with relaxation frequency one order lower than that of the Goldstone mode. The nature of this mode, contributing for both $S_{C_{FI1}}^*$ and S_C^* phases, is not understood. It cannot be related to the antiphase azimuthal mode [6], responsible for the $S_{C_A}^*$–$S_{C_{FI}}^*$ phase transition for the compound $n = 9$ [3] which exhibits a maximal contribution at this transition. In the ferroelectric S_C^* phase, the contribution of the Goldstone mode for the compound with $n = 11$ is about five times lower in comparison with the compounds with $n = 9$, 10 or 12. This result seems to indicate a clear change in the elastic properties of this compound, but the values of the spontaneous polarization, which were checked for the whole series of compounds, were similar.

In the antiferro- and ferri-electric phases, a high frequency mode has been detected and may be related either to the rotation of molecules around their short

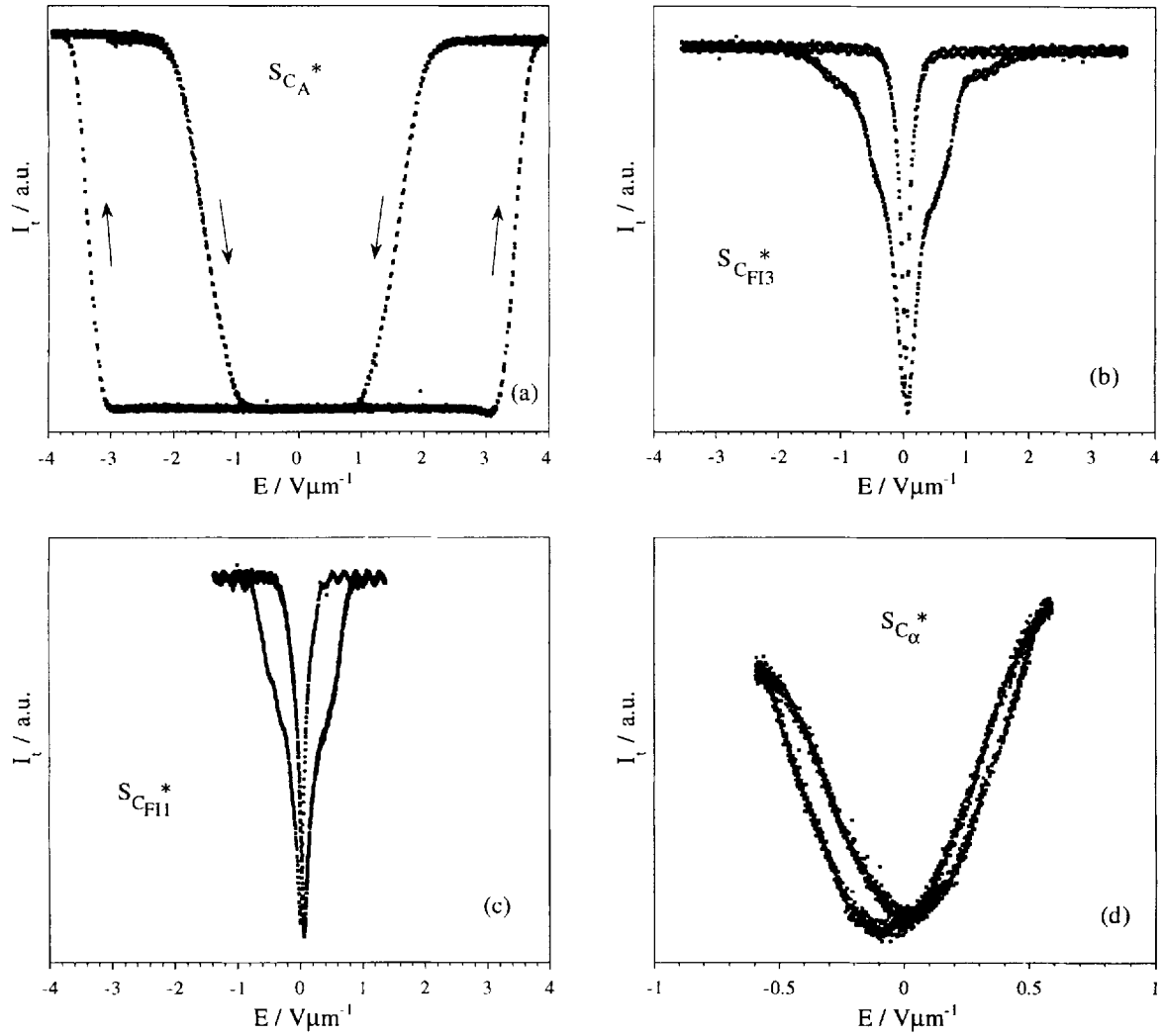

Figure 7. Optical hysteresis loops recorded for 12FHTBBM7* at (*a*) 71°C, (*b*) 94°C, (*c*) 98°C and (*d*) 118·5°C. The phases are indicated for each loop.

axes or to the non-collective azimuthal mode. Such a mode was also found for the compound $n = 9$ [3].

In the compounds $n = 9$, 10, 11 and 12 of this series, the $S^*_{C_\alpha}$ phase was identified between the S^*_C and the S_A phases. The existence of a mode, probably triggered by the softening of the molecular tilt at the $S^*_{C_\alpha}$–S_A transition, is supposed to be characteristic of the $S^*_{C_\alpha}$ phase. The contribution of this mode is temperature dependent and is maximal at the S^*_C–$S^*_{C_\alpha}$ phase transition [2, 3]. A similar contribution, exhibiting a maximum at the $S^*_{C_A}$–$S^*_{C_\alpha}$ phase transition was also reported for the mixture of MHPOOCBC with EHPOCBC in reference [9].

The phase sequences of the compounds $n = 9$, 10, 11 and 12 are presented in figure 9; the transition temperatures were obtained from heating runs. One can see that the temperatures of both S^*_C–$S^*_{C_\alpha}$ and $S^*_{C_\alpha}$–S_A phase transitions increase with the alkoxy chain length, while the S_A–I transition temperatures fall. Therefore, the stability interval of the S_A phase decreases with increasing n. For the compounds $n = 9$ and $n = 10$, only one ferrielectric phase occurs, in contrast to the compounds $n = 11$ and $n = 12$ where three and two ferrielectric phases seem to exist, respectively [3, 4].

Figure 9 clearly shows that the temperature range of the S^*_C phase is larger for the compound $n = 9(11)$ than for the compound $n = 10(12)$. On the other hand, an opposite situation is observed for the temperature range of the $S^*_{C_A}$ phase. Such behaviour can be interpreted as an increase in interlayer interactions that stabilize the antiferroelectric molecular order relatively to the ferroelectric interactions. This odd and even effect of the alkoxy chain on the existence and on the temperature range of the S^*_C and $S^*_{C_A}$ phases has already been observed in another thiobenzoate series [1].

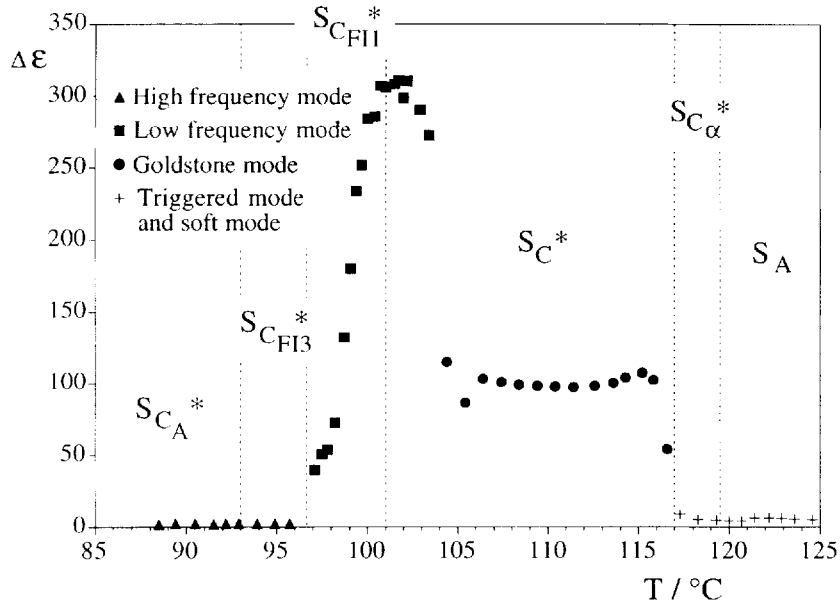

Figure 8. Dielectric relaxation strength $\Delta\varepsilon$ for modes contributing to the dielectric constant in the polar phases and in the S_A phase of 12FHTBBM7*, on heating. The line corresponding to the $S^*_{C_A}$–$S^*_{C_{FI3}}$ phase transition was taken from figure 6.

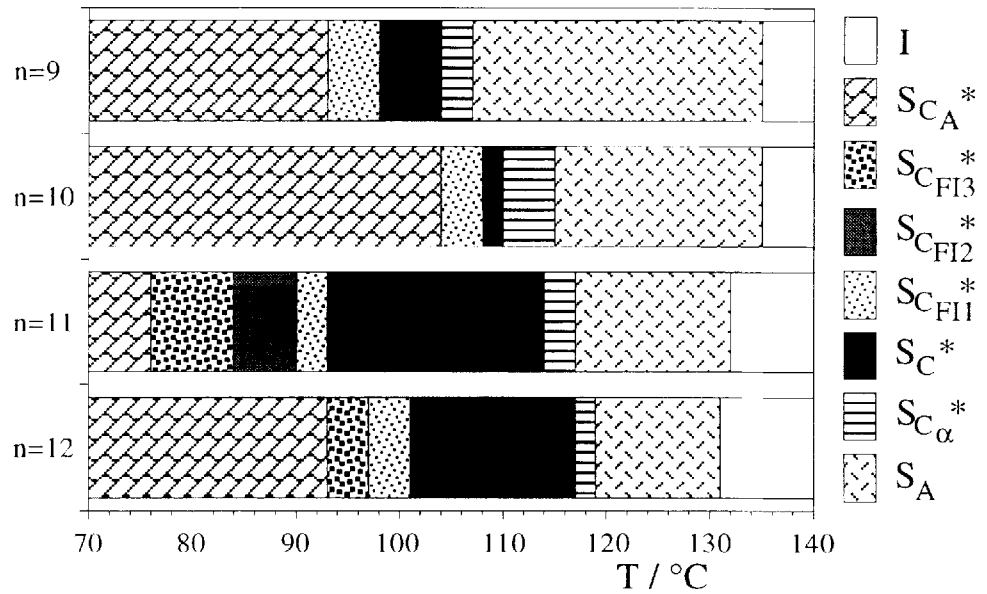

Figure 9. Phase diagrams for the series of compounds *n*FHTBBM7* between 70 and 140°C. The transition temperatures were obtained for increasing temperatures. The results for $n = 9$ and $n = 10$ were taken from references [3] and [4], respectively. For $n = 11$ and $n = 12$, the temperature ranges of the $S^*_{C_{FI3}}$ and $S^*_{C_\alpha}$ phases were taken from TSM and DSC measurements, respectively.

In reference [9] it has been shown that for a system obtained by mixing two compounds, one exhibiting only the antiferroelectric phase and the other only the ferroelectric phase, one or more ferrielectric phases appear. When both interactions are well balanced and moderate in strength, the competition between ferroelectric and antiferroelectric interactions results in the onset of such ferrielectric phases [10]. In the present work, a similar effect is observed for the series of compounds *n*FHTBBM7*, as the ferroelectric and antiferroelectric interactions are nearly balanced. A slight change of the interlayer interactions by increasing the length of the alkoxy chain can then bring about a rather drastic change in the polar phase sequence.

The authors are deeply indebted to Albano Costa for technical assistance. This work was partially supported by JNICT and by the Service Culturel Scientifique et de Coopération de l'Ambassade de France au Portugal. One of us (M. G.) is grateful to JNICT for the grant PRAXIS XXI/BCC/4377/94.

References

[1] NGUYEN, H. T., ROUILLON, J. C., CLUZEAU, P., SIGAUD, G., DESTRADE, C., and ISAERT, N., 1994, *Liq. Cryst.*, **17**, 571.

[2] GLOGAROVÁ, M., SVERENYAK, H., NGUYEN, H. T., and DESTRADE, C., 1993, *Ferroelectrics*, **147**, 43.

[3] SIMEÃO CARVALHO, P., CHAVES, M. R., DESTRADE, C., NGUYEN, H. T., and GLOVAROVÁ, M., *Liq. Cryst.* (in press).

[4] DESTRADE, C., SIMEÃO CARVALHO, P., and NGUYEN, H. T., 1996, *Ferroelectrics*, **177**, 161.

[5] SIMEÃO CARVALHO, P., GLOGAROVÁ, M., CHAVES, M. R., DESTRADE, C., and NGUYEN, H. T., *Liq. Cryst.* (to be published).

[6] GISSE, P., PAVEL, J., NGUYEN, H. T., and LORMAN, V. L., 1993, *Ferroelectrics*, **147**, 27.

[7] (*a*) LEVSTIK, A., CARLSSON, T., FILIPIC, C., and ZEKS, B., 1987, *Phys. Rev. A*, **35**, 3527; (*b*) GOODBY, J. W., BLINC, R., CLARK, N. A., LAGERWALL, S. T., OSIPOV, M. A., PIKIN, S. A., SAKURAI, T., YOSHINO, K., and ZEKS, B., 1991, *Ferroelectric Liquid Crystals—Principles, Properties and Applications* (Gordon and Breach), pp. 377–387.

[8] HIRAOKA, K., TAKEZOE, H., and FUKUDA, A., 1993, *Ferroelectrics*, **147**, 13.

[9] ISOZAKI, T., FUJIKAWA, T., TAKEZOE, H., FUKUDA, A., HAGIWARA, T., SUZUKI, Y., and KAWAMURA, I., 1993, *Phys. Rev. B*, **48**, 13439.

[10] FUKUDA, A., TAKANISHI, Y., ISOZAKI, T., ISHIKAWA, K., and TAKEZOE, H., 1994, *J. Mater. Chem.*, **4**, 997.